

SEMI-ANNUAL STATUS REPORT

Submitted to: NASA Marshall Space Flight Center

Grant Title: Theory and Computation of Optimal Low- and Medium-Thrust Transfers

Grant Number: NAG8-921

Principal Investigator /Project Director: Dr. C.-H. Chuang
School of Aerospace Engineering
Georgia Institute of Technology
Atlanta, GA 30332-0150
(404) 894-3075

191651
191651
191651
P- 34

Research Assistant: Troy Goodson
School of Aerospace Engineering
Georgia Institute of Technology

Period Covered: July 7, 1992 to January 6, 1993

Date of Submission: January 5, 1993

(NASA-CR-191651) THEORY AND
COMPUTATION OF OPTIMAL LOW- AND
MEDIUM-THRUST TRANSFERS Semiannual
Status Report, 7 Jul. 1992 - 6 Jan.
1993 (Georgia Inst. of Tech.)
34 p

N93-16428

Unclas

G3/20 0137562

TABLE OF CONTENTS

	SUMMARY OF THE RESEARCH RESULTS.....	ii
	ABSTRACT.....	1
I.	INTRODUCTION	1
II.	THE PROBLEM.....	3
III.	THE FIRST-ORDER NECESSARY CONDITIONS.....	8
	III.1. THE HAMILTONIAN	10
	III.2. THE COSTATES.....	13
IV.	SOLVED PROBLEMS	14
	IV.1. SIMPLIFICATIONS.....	14
	IV.2. THE TWO-POINT BOUNDARY VALUE PROBLEM.....	15
	IV.3. NON-DIMENSIONALIZATION	17
	IV.4. ATMOSPHERE MODEL.....	19
	IV.5. THE MULTIPLE POINT SHOOTING METHOD OF BOUNDSCO	20
	IV.6. THE MINIMIZING-BOUNDARY-CONDITION METHOD	21
	IV.7. SAMPLE PROBLEMS AND SOLUTIONS	21
V.	CONCLUSIONS	23
	REFERENCES	24

SUMMARY OF RESEARCH RESULTS

1. The following report titled "Computation of Optimal Low- and Medium- Thrust Orbit Transfers" gives the detail of the research results. We summary these results and future research plan here.
2. The first-order necessary conditions for a general final mass maximization problem has been set up. In the problem formulation we include second-harmonic oblateness, atmospheric drag, and allow three-dimensional, non-coplanar, non-aligned elliptic orbits. In order to ease the numerical calculation we transform the original free final-time problem to a fixed final-time problem, and non-dimensionalize the state variables.
3. Although we can use the constant angular momentum equation, the conservative energy equation, and the orbit equation to specify the boundary conditions for the terminal orbit, we notice that this set of boundary conditions does not uniquely determine an orbit. This is due to the fact that for a given point in space we can have two different velocity vectors (difference in direction only) and yet have the same angular momentum and energy. Proper boundary conditions should be three eccentricity vector equations plus three angular momentum vector equations. Since both eccentricity and angular momentum equations specify the same orbit plane, one of these equations is redundant. That is for a three dimensional problem we only need five equations out of both sets of equations. For two dimensional problem we need two eccentricity equations and one angular momentum equation.
4. We have applied two indirect optimization methods: BOUNDSCO and MBCM (minimizing-boundary-condition method) successfully to several simplified examples. The examples are two dimensional with oblateness effect and atmospheric drag force. Both methods converge to the solutions with about the same sensitivity in the initial guess. Although we have more freedom in selecting the initial guess at every node points, BOUNDSCO does not adjust the number of switching points and the switching pattern during the iteration. On the other hand, MBCM implements the switching function into the integrator and adjust the switching points and the switching pattern automatically during the iteration.
5. Our current plan is to combine advantageous features of BOUNDSCO and MBCM into a new algorithm. The new algorithm will use the idea of the multiple-point shooting method to spread the unknowns among the node points, and between two node points applies the minimizing-boundary-condition method.
6. There is still a question about the local optimum or global optimum for free final time problem. We have some difficulty in converging the transversality condition for the free final time case. In Edelbaum's paper, he shows that three impulses control is usually minimum. However, such claim for low and

medium thrust has not been shown anywhere. Our current hypothesis suggests that the global minimum solution will be at infinite final time and local minimum solutions exist for finite final time. We expect to answer this question by obtaining all the local minimum solutions (if they exist) and compare their cost functions along the final time axis.

Computation of Optimal Low- and Medium-Thrust Orbit Transfers

ABSTRACT

This report presents the formulation of the optimal low- and medium-thrust orbit transfer control problem and methods for numerical solution of the problem. The problem formulation is for final mass maximization and allows for second-harmonic oblateness, atmospheric drag, and three-dimensional, non-coplanar, non-aligned elliptic terminal orbits. We setup some examples to demonstrate the ability of two indirect methods to solve the resulting TPBVPs.

The methods demonstrated are the multiple-point shooting method as formulated in H. J. Oberle's subroutine BOUNDSCO, and the minimizing boundary-condition method (MBCM). We find that although both methods can converge solutions, there are trade-offs to using either method. BOUNDSCO has very poor convergence for guesses that do not exhibit the correct switching structure. MBCM, however, converges for a wider range of guesses. However, BOUNDSCO's multi-point structure allows more freedom in guesses by increasing the node points as opposed to only guessing the initial state in MBCM. Finally, we note an additional drawback for BOUNDSCO: the routine does not supply information to the users routines for switching function polarity but only the location of a preset number of switching points.

I. INTRODUCTION

The ability to perform any given orbit transfer with a minimum use of fuel is obviously desirable. Useful solutions to this problem will account for

at least some approximation to real-life. Therefore, a formulation that includes second-harmonic oblateness and atmospheric drag will be useful.

This report follows such a derivation all the way through to the establishment of a two-point boundary-value problem for optimal low- and medium- thrust orbit transfer. The core cost function is defined simply as the final mass of the spacecraft plus fuel, setting the tone for the maximization problem. The differential constraint is thoroughly defined in terms of the oblateness model and an assumed atmosphere model.

The thrust (control) appears linear in the differential constraint. This results in bang-bang control or singular-arc solutions for the final mass maximization problem. Although bang-bang control is assumed here the possibility of having a singular arc has not been ruled out for a general case. In order to ensure the singular arc solution does not occur, we check the derivative of the switching function at each switching point. However, when our programs reach a non-optimal solution high frequency chattering solutions do occur occasionally. This could indicate that singular-arc solutions are possible for some modification of system parameters and models.

The final mass maximization problem should be a free final time optimal control problem. For impulsive thrust, the Hohmann transfer gives minimum fuel but maximum transfer time. Although the three-impulse Hohmann transfer performs better than a two-impulse Hohmann transfer, Edelbaum¹ shows that the number of impulses may be finite for a global minimum. for low- and medium-thrust orbit transfer the same conclusion has not be shown anywhere. One hypothesis is that the global minimum will be at infinite final time and local minimum solutions exist for finite final time. In other words, this assumes for a given number of switching points (must be at least two) there is a local minimum with finite final time. We do have difficulties in converging the transversality condition corresponding to optimal final time.

We present solutions to three specific optimization problems. These solutions represent the ability of the two TPBVP solvers. The methods

considered are (1) BOUNDSCO, a multi-point shooting algorithm devised by H. J. Oberle and (2) the minimizing boundary-condition method (MBCM), a modification to the shooting method devised by the authors of ref(9).

Both methods converge solutions for about equal sensitivity in initial guesses. In order to achieve the same accuracy along the path, BOUNDSCO needs to converge the boundary conditions at every node point to the same accuracy as the integration routine. The number of switching points and the switching pattern need to be assumed and stay unchanged when BOUNDSCO is used. On the other hand, MBCM does not constrain the number of switching points and MBCM updates the switching pattern along the integrated path.

II. THE PROBLEM

The problem discussed herein is the following: maximize the final mass of a thrusting spacecraft for a given orbital transfer. The craft can be considered as under the influence of some planet's gravitational field and atmospheric drag. The thrust of the spacecraft is limited between zero and some T_{\max} . The transfer will be defined by the terminal orbits. Solutions are sought for both fixed and free final time problems and both the case of fixed and free terminal points.

II. 1. *The Cost Functional*

The core cost functional must be defined. We shall define the cost as

$$J = m(t_f) \quad (1)$$

where $m(t_f)$ represents the mass of the spacecraft plus its fuel at the end of the orbital transfer. We shall use the methods of optimal control to maximize the cost functional, thereby maximizing the final mass and solving the problem.

II. 2. *Differential constraint: System Dynamics*

We represent the spacecraft by a point mass and assume it to be a thrusting craft acted upon by the aerodynamic drag and oblate-body gravity forces of a central body. We also represent the central body, or planet, as a point mass positioned at its own center of gravity. We restrict the problem to crafts of mass much smaller than that of the central body, allowing us to fix the planet in inertial space. We shall describe this inertial space with a rectangular Cartesian inertial reference frame. All motion within this frame of reference agreeing with the above assumptions must satisfy the well-known Newton's equation:

$$\vec{F} = \frac{d(m\vec{v})}{dt} \quad (2)$$

where m is the spacecraft mass and \vec{v} is its velocity with respect to the reference frame.

In this case, gravity, drag, and thrust make up the total force acting on the craft. The thrust on the craft is composed of two separated thrusts, the pressure thrust and the thrust created by the expulsion of mass. That is,

$$\vec{F} \equiv \vec{F}_{\text{pressure thrust}} - \vec{F}_{\text{drag}} - \vec{F}_{\text{gravity}} = m\dot{\vec{v}} - \dot{m}\vec{v}_e \quad (3)$$

where \vec{v}_e is the expulsive velocity of mass. Therefore,

$$\vec{F}_{\text{total thrust}} \equiv \vec{F}_{\text{pressure thrust}} + \dot{m}\vec{v}_e \quad (4)$$

and

$$m\dot{\vec{v}} = \vec{F}_{\text{thrust}} - \vec{F}_{\text{drag}} - \vec{F}_{\text{gravity}} \quad (5)$$

We write the total thrust, herein referred to as just thrust, as some time-varying magnitude, T , independent of a time-varying direction, \vec{e} :

$$\vec{F}_{\text{thrust}} = T \vec{e} \quad (6)$$

Note that \vec{e} is expressed as a unit vector. For a three dimensional thrust vector the control requires three components. For two dimensional problems only two independent control components are required.

The mass will decrease according to

$$\dot{m} = -\frac{T}{g_0 I_{sp}} \quad (7)$$

We assume that the atmosphere surrounding the central body can be described by an exponential model of the standard atmosphere². The following equation³ describes such a drag force:

$$\vec{F}_{\text{drag}} = \frac{1}{2} \rho_0 e^{-\beta(r-r_0)} S C_D \frac{|\vec{v}|^2}{|\vec{v}|} = \frac{1}{2} \rho_0 e^{-\beta(r-r_0)} S C_D |\vec{v}| \vec{v} \quad (8)$$

where β and r_0 are constants from the atmosphere model describing air density variation in the prescribed altitude region, ρ_0 is the atmosphere density for the altitude r_0 , S is the wetted area of the craft, C_D is the craft's drag coefficient, and \vec{v} is craft's current velocity with respect to the inertial reference frame. We are assuming that no matter the orientation of the craft the product of SC_D remains the same and that the craft always remains in a region where the chosen exponential atmosphere model is valid.

Within the confines of this study, the only other influence on the craft is gravitational potential energy. The gravitational potential energy to the second harmonic is⁴:

$$U = -\frac{m\mu}{r} - \frac{1}{3} J R^2 \frac{m\mu}{r^3} (1 - 3 \cos^2\theta) \quad (9)$$

Where R is the equatorial radius of the central body, θ is the latitude angle of the current position from the equator, and r is the distance from the central

body's center of gravity to the current position of the craft with respect to the inertial reference frame, μ is the gravitational constant for the central body, m is the mass of spacecraft, and J is a constant describing the mass distribution of the planet. There are additional mass distribution terms but we shall truncate the series here.

We now assume that (1) the central body is fixed at the center of the reference frame and (2) that the plane of the central body's equator is aligned with the x-y plane. The assumption (1) means that the position, velocity, and acceleration of the craft are now measured with respect to the central body. The assumption (2) means that we may describe r with Cartesian coordinates by

$$r = \sqrt{x^2 + y^2 + z^2} \quad (10)$$

and we may describe θ with Cartesian coordinates by

$$z = r \cos \theta \quad (11)$$

We may now write the gravitation potential as

$$U = -\frac{m\mu}{r} - \frac{1}{3} J R^2 \frac{m\mu}{r^3} \left(1 - 3\left(\frac{z}{r}\right)^2\right) \quad (12)$$

The force experienced by moving in a potential field U is $\frac{\partial U}{\partial \vec{r}}$.

Performing this operation on the gravitational potential yields

$$\vec{F}_{\text{gravity}} = \left(\frac{\partial U}{\partial \vec{r}}\right)^T \quad (13)$$

and

$$\frac{\partial U}{\partial x} = \frac{m\mu}{r^3} x + JR^2 \frac{m\mu}{r^5} x (1 - 5\left(\frac{z}{r}\right)^2) \quad (14)$$

$$\frac{\partial U}{\partial y} = \frac{m\mu}{r^3} y + JR^2 \frac{m\mu}{r^5} y (1 - 5\left(\frac{z}{r}\right)^2) \quad (15)$$

$$\frac{\partial U}{\partial z} = \frac{m\mu}{r^3} z + JR^2 \frac{m\mu}{r^5} z (3 - 5\left(\frac{z}{r}\right)^2) \quad (16)$$

All of the dynamics combines to form the following equations of motion

$$m\ddot{x} = T e_x - \frac{m\mu}{r^3} x - JR^2 \frac{m\mu}{r^5} x (1 - 5\left(\frac{z}{r}\right)^2) - \frac{1}{2} \rho_0 e^{-\beta(r-r_0)} S C_D v \dot{x} \quad (17a)$$

$$m\ddot{y} = T e_y - \frac{m\mu}{r^3} y - JR^2 \frac{m\mu}{r^5} y (1 - 5\left(\frac{z}{r}\right)^2) - \frac{1}{2} \rho_0 e^{-\beta(r-r_0)} S C_D v \dot{y} \quad (17b)$$

$$m\ddot{z} = T e_z - \frac{m\mu}{r^3} z - JR^2 \frac{m\mu}{r^5} z (3 - 5\left(\frac{z}{r}\right)^2) - \frac{1}{2} \rho_0 e^{-\beta(r-r_0)} S C_D v \dot{z} \quad (17c)$$

which can be written in vector-matrix form as

$$\ddot{\mathbf{r}} = \frac{T}{m} \hat{\mathbf{e}} - \frac{\mu}{r^3} \hat{\mathbf{r}} - \left\{ JR^2 \frac{\mu}{r^5} \begin{bmatrix} 1 - 5\left(\frac{z}{r}\right)^2 & 0 & 0 \\ 0 & 1 - 5\left(\frac{z}{r}\right)^2 & 0 \\ 0 & 0 & 3 - 5\left(\frac{z}{r}\right)^2 \end{bmatrix} \hat{\mathbf{r}} - \frac{1}{2} \frac{\rho_0}{m} e^{-\beta(r-r_0)} S C_D v \dot{\mathbf{r}} \right\} \quad (18)$$

To conform to convention we make the change from J to J_2 as described in ref(4):

$$\ddot{\mathbf{r}} = \frac{\mathbf{I}}{m} \ddot{\mathbf{e}} - \frac{\mu}{r^3} \dot{\mathbf{r}} - \left\{ \frac{3}{2} \mu J_2 \frac{R^2}{r^5} \begin{bmatrix} 1 & 0 & 0 \\ 0 & 1 & 0 \\ 0 & 0 & 3 \end{bmatrix} - 5 \left(\frac{\mathbf{z}}{r} \right)^2 \right\} \dot{\mathbf{r}} - \frac{1}{2} \frac{\rho_0}{m} e^{-\beta(r-r_0)} S C_D \mathbf{v} \dot{\mathbf{r}} \quad (19)$$

This can also be rewritten as a first-order system:

$$\dot{\mathbf{r}} = \mathbf{v} \quad (20a)$$

$$\dot{\mathbf{v}} = \frac{\mathbf{I}}{m} \ddot{\mathbf{e}} - \frac{\mu}{r^3} \dot{\mathbf{r}} - \left\{ \frac{3}{2} \mu J_2 \frac{R^2}{r^5} \begin{bmatrix} 1 & 0 & 0 \\ 0 & 1 & 0 \\ 0 & 0 & 3 \end{bmatrix} - 5 \left(\frac{\mathbf{z}}{r} \right)^2 \right\} \dot{\mathbf{r}} - \frac{1}{2} \frac{\rho_0}{m} e^{-\beta(r-r_0)} S C_D \mathbf{v} \dot{\mathbf{v}} \quad (20b)$$

III. THE FIRST-ORDER NECESSARY CONDITIONS

All problems herein perform a maximization of the final mass. Now, in order to write the adjointed cost functional we need to know what is included in the state, in the control, and what the constraints on these are.

First, however, we note that the problems herein are also free-final-time problems. The three differential equations above are written with respect to the independent variable t (time). For ease in numerical methods, we want to transfer the problem from free- to fixed- final time. This means that we must define a new independent variable τ (non-dimensional time) to be used in the place of t (dimensional time). This allows t_f to become a state variable. We make the following scaling:

$$t = t_f \tau \quad (21)$$

Therefore, to translate this to a fixed-time problem, t_f must multiply the derivatives of the states. The dot above a variable now means a derivative with respect to τ .

We know what to include in the state, $\vec{\mathbf{x}}(\tau)$:

$$\vec{x}(\tau) = \begin{bmatrix} \vec{r}^T(\tau) & \vec{v}^T(\tau) & m(\tau) & t_f \end{bmatrix}^T \quad (22)$$

We also know that our state is confined by the system dynamics so that

$$\dot{\vec{x}}(\tau) = \begin{bmatrix} \vec{v} \\ \frac{T}{m} \vec{e} - \frac{\mu}{r^3} \vec{r} - \left\{ \frac{3}{2} \mu J_2 \frac{R^2}{r^5} \left(\begin{bmatrix} 1 & 0 & 0 \\ 0 & 1 & 0 \\ 0 & 0 & 3 \end{bmatrix} - 5 \left(\frac{\vec{z}}{r} \right)^2 \right) \right\} \vec{r} - \frac{1}{2} \frac{\rho_0}{m} e^{-\beta(\tau - \tau_0)} S C_D \vec{v} \\ -\frac{T}{g_0 I_{sp}} \\ 0 \end{bmatrix} \quad (23)$$

for all time $\tau \in [0,1]$. This is the differential constraint of the control problem.

The thrust magnitude has both an upper and a lower bound. The upper bound we shall call T_{\max} , the lower bound is obviously zero. We, therefore, also have an inequality constraint that must be satisfied for all time $\tau \in [0,1]$:

$$(T - T_{\max})T \leq 0 \quad (24)$$

and Eqn (25) can be rewritten as an equality constraint

$$(T - T_{\max})T + \alpha^2 = 0 \quad (25)$$

where α is a slack variable, free to change with time. Finally, we need to specify the terminal orbits. We will do so by writing a vector equation

$$\vec{\psi}(\vec{x}(0), \vec{x}(1)) = 0 \quad (26)$$

that is only satisfied when our initial and final states both lie on their respective orbits.

Now we know enough to write the adjoined cost functional for this problem:

$$J = m(1) + \vec{v}^T \vec{\psi}(\vec{x}(0), \vec{x}(1)) + \int_0^1 \left\{ \vec{\lambda}^T [\vec{f}(\vec{x}(t), \vec{u}(t)) - \dot{\vec{x}}] + \mu[(T - T_{\max})T + \alpha^2] \right\} dt \quad (27)$$

where $m(1)$ is the final mass and $\vec{\psi}(\vec{x}(0), \vec{x}(1)) = 0$ represents the boundary conditions.

The $\vec{\lambda}$ shown in the cost functional is the costate vector, also called the Lagrange multipliers. This vector will be of the same dimensions as the state. For simplification's sake, we will segment this vector as follows:

$$\vec{\lambda}(t) = \begin{bmatrix} \vec{\lambda}_r^T(t) & \vec{\lambda}_v^T(t) & \lambda_m(t) & \lambda_{t_f} \end{bmatrix}^T \quad (28)$$

Also, in Eqn (27), \vec{v} is the Lagrange multiplier corresponding to the boundary conditions $\vec{\psi}$. \vec{v} is a constant in time.

III.1. The Hamiltonian

With the pertinent dynamics defined, we are now able to write the Hamiltonian for the system. We take the Hamiltonian from the cost functional as

$$H(\vec{x}(t), \vec{u}(t)) = \vec{\lambda}^T [\vec{f}(\vec{x}(t), \vec{u}(t))] + \mu[(T - T_{\max})T + \alpha^2] \quad (29)$$

A major simplification can be made now. Notice that, excluding the constraint on the thrust, the Hamiltonian is linear with respect to the control T (but we shall see it is not linear with respect to \vec{e}):

$$H(\vec{x}(t), \vec{u}(t)) = \frac{T}{m} \lambda_v^{-T} \vec{e} - \lambda_m \frac{T}{g_0 I_{sp}} + \dots \quad (30)$$

This, in conjunction with the structure of the thrust constraint, means that we may assume that this is a 'bang-bang' control problem. Enough is known about this type of problem so that we may do the following:

(1) Define a new Hamiltonian that differs from the original only in the omission of the thrust constraint.

$$H(\vec{x}(t), \vec{u}(t)) = \lambda^T [f(\vec{x}(t), \vec{u}(t))] \quad (31)$$

(2) Establish what will be called the switching function. In general, the switching function is defined by the partial derivative of the Hamiltonian with respect to the control by which it is linear. For this problem, This is done by evaluating $\frac{\partial H}{\partial T}$:

$$\frac{\partial H}{\partial T} = H_T = \frac{\lambda_v^{-T} \vec{e}}{m} - \frac{\lambda_m}{I_{sp} g_0} \quad (32)$$

This, Eqn (32), is the switching function.

(3) Evaluate a restricted case of the well-known Euler-Lagrange equations. Most of these determine the costate dynamics and we shall see these in section III.2, however, the last one determines part of the control for the problem. This equation is

$$\frac{\partial H}{\partial \vec{e}} = 0 \quad (33)$$

Evaluating (33), it appears that H is linear with respect to \vec{e} . However, we must remember that \vec{e} represents only the direction of the thrust. If we

exchange \vec{e} for some angle θ and define this angle as between \vec{e} and $\vec{\lambda}_v$ we may write

$$H = \frac{I}{m} \vec{\lambda}_v^T \vec{e} + \dots = \frac{I}{m} |\vec{\lambda}_v| |\vec{e}| \cos \theta + \dots \quad (34)$$

$$H = \frac{I}{m} |\vec{\lambda}_v| \cos \theta + \dots \quad \text{since } |\vec{e}| = 1 \quad (35)$$

Evaluating H_θ we find that

$$\frac{\partial H}{\partial \theta} = -\frac{I}{m} |\vec{\lambda}_v| \sin \theta \quad (36)$$

and this equals zero only when the vectors are parallel. There are only two choices for \vec{e} : in the direction of $\vec{\lambda}_v$ or in the exact opposite direction. Since we are maximizing the final vehicle mass, we need to have $H_{\theta\theta}$ negative (one of the sufficient conditions for the second variation). This is only satisfied with \vec{e} in the direction of $\vec{\lambda}_v$ or

$$\vec{e} = \frac{\vec{\lambda}_v}{|\vec{\lambda}_v|} \quad (37)$$

We must obey this for all time $\tau \in [0,1]$. This result is consistent with that of Lawden's primer vector⁵.

(4) Perform bang-bang control with T . This means that T is always on-boundary, i.e. $T=0$ or $T=T_{\max}$ at any $\tau \in [0,1]$. We know which value to use for T by evaluating the switching function, which we can now write as

$$H_T = \frac{|\vec{\lambda}_v|}{m} - \frac{\lambda_m}{I_{sp} g_0} \quad (38)$$

The bang-bang control law is

$$\begin{aligned} H_T \geq 0 & \quad T = T_{\max} \\ H_T < 0 & \quad T = 0 \end{aligned} \quad (39)$$

This switching structure satisfies the Pontryagin maximum principle by maximizing the Hamiltonian using T .

III.2. The Costates

The costate dynamics can be found from the following Euler-Lagrange equations, relating them to the Hamiltonian:

$$\dot{\lambda}_r = -\frac{\partial H^T}{\partial \vec{r}} \quad (40)$$

$$\dot{\lambda}_v = -\frac{\partial H^T}{\partial \vec{v}} \quad (41)$$

$$\dot{\lambda}_m = -\frac{\partial H}{\partial m} \quad (42)$$

To evaluate these, we must first substitute the equations of motion into the Hamiltonian

$$\begin{aligned} H = & \int_0^T \left\{ \lambda_r^T \vec{v} + \lambda_v^T \left[\frac{T}{m} \vec{e} - \left[\frac{\mu}{r^3} + \frac{3}{2} J_2 \frac{\mu}{r^5} R^2 \bar{N} - \right. \right. \right. \\ & \left. \left. \left. - \frac{15}{2} J_2 \frac{\mu}{r^7} R^2 (z^2) \right] \vec{r} - \frac{1}{2} \frac{\rho_0}{m} e^{-\beta (r-r_0)} S C_D v \vec{v} \right] \right. \\ & \left. + \lambda_m \frac{T}{g_0 I_{sp}} \right\} \end{aligned} \quad (43)$$

When evaluated, these become the following vector and scalar differential equations:

$$\begin{aligned} \dot{\vec{\lambda}}_r = & \text{tr} \left\{ \mu \left[\frac{\vec{\lambda}_v}{r^3} - 3 \frac{(\vec{\lambda}_v^T \vec{r}) \vec{r}}{r^5} \right] - \frac{1}{2} \frac{\rho_0 \beta}{m r} e^{-\beta(r-r_0)} S C_D v (\vec{\lambda}_v^T \vec{v}) \vec{r} \right. \\ & \left. + \frac{3}{2} J_2 \mu R^2 \left[\frac{\vec{N} \vec{\lambda}_v}{r^5} - 5 \frac{(\vec{\lambda}_v^T \vec{N} \vec{r}) \vec{r}}{r^7} \right] - \frac{15}{2} J_2 \mu R^2 \left[\frac{z^2}{r^7} \vec{\lambda}_v - (\vec{\lambda}_v^T \vec{r}) \left(\frac{7z^2}{r^9} \vec{r} - \frac{2z}{r^7} \vec{k} \right) \right] \right\} \end{aligned} \quad (44)$$

where $\vec{k} = \begin{bmatrix} 0 \\ 0 \\ 1 \end{bmatrix}$

$$\dot{\vec{\lambda}}_v = \text{tr} \left[-\vec{\lambda}_r^T + \frac{1}{2} \frac{\rho_0}{m} e^{-\beta(r-r_0)} S C_D \left(\vec{\lambda}_v v + \frac{(\vec{\lambda}_v^T \vec{v}) \vec{v}}{v} \right) \right] \quad (45)$$

$$\dot{\lambda}_m = \text{tr} \left[-\frac{1}{m^2} \vec{\lambda}_v^T \vec{e} + \frac{1}{2} \frac{\rho_0}{m^2} e^{-\beta(r-r_0)} S C_D v \vec{\lambda}_v^T \vec{v} \right] \quad (46)$$

IV. SOLVED PROBLEMS

IV.1. Simplifications

We have made a few simplifications that ease the formulation of the numerical problem and its solution. The first of these is the reduction from a three-dimensional problem to a two-dimensional problem. To remove this dimension, we simply remove the z-component to all equations. Because of the chosen coordinate system, this also means that all orbit transfers considered are equatorial. Unfortunately, the effect of oblateness is substantially decreased for this case. The other simplification is the restriction

of problems to fixed-initial points. This also greatly eases the problem formulation. The third and final simplification is the fixing of the final time.

IV.2. The Two-Point Boundary Value Problem

As a result of the simplifications, the boundary conditions have been stated in two dimensions. The starting orbit determines the initial conditions on position and velocity. The final conditions, however, require a more abstract specification as we do not know exactly at what point the craft will enter this orbit. The following relations specify the final orbit: (All of the following conditions is to be evaluated at the final time, t_f , or $\tau=1$.)

$$\text{(Angular Momentum) } \psi_1: \left\{ \begin{array}{l} \vec{R} \times \vec{V} = \vec{H} \\ \langle x, y \rangle \times \langle u, v \rangle = xv - yu = h \\ xv - yu - h = 0 \end{array} \right\} \quad (47a)$$

$$\text{(eccentricity vector (x)) } \psi_2: \left\{ \begin{array}{l} e_x = \frac{1}{\mu} \left[\left(v^2 - \frac{m}{r} \right) x - (\vec{r}^T \vec{V}) u \right] \\ \frac{1}{\mu} \left[\left(v^2 - \frac{m}{r} \right) x - (\vec{r}^T \vec{V}) u \right] - e_x = 0 \end{array} \right\} \quad (47b)$$

$$\text{(eccentricity vector (y)) } \psi_3: \left\{ \begin{array}{l} e_y = \frac{1}{\mu} \left[\left(v^2 - \frac{m}{r} \right) y - (\vec{r}^T \vec{V}) v \right] \\ \frac{1}{\mu} \left[\left(v^2 - \frac{m}{r} \right) y - (\vec{r}^T \vec{V}) v \right] - e_y = 0 \end{array} \right\} \quad (47c)$$

Note that the orbit equation for x-axis aligned orbits and the energy equation can replace (47b) and (47c). However, the combined constraints of angular, momentum, orbit, and energy equations do not uniquely specify an

x-axis aligned final orbit. There are two possible velocity vectors at one point with the same angular momentum and energy.

These conditions completely determine the final orbit. However, these conditions do not complete the two-point boundary-value problem. To complete the TPBVP, the methods of optimal control supply use with a set of natural boundary conditions found by evaluating

$$\vec{\lambda}(1) = \left(\frac{\partial G}{\partial \vec{x}(1)} \right)^T \quad (48)$$

where G is the constructed from the function portion of the cost functional, e.g. for the cost functional

$$J = m(1) + \vec{v}^T \vec{\psi}(\vec{x}(0), \vec{x}(1)) + \int_0^1 \left\{ \vec{\lambda}^T [\dot{\vec{f}}(\vec{x}(t), \vec{u}(t)) - \dot{\vec{x}}] + \mu [(T - T_{\max})T + \alpha^2] \right\} dt \quad (49)$$

G is

$$G = m(1) + \vec{v}^T \vec{\psi}(\vec{x}(0), \vec{x}(1)) \quad (50)$$

Constructing G with the above conditions on the states, we can find conditions on the costates at $\tau=1$:

$$G = m + v_1 (x v - y u - h) + [v_2 \quad v_3] \left[\frac{1}{\mu} \left((v^2 - \frac{m}{r}) \dot{r} - (\dot{r}^T \vec{V}) \vec{V} \right) - \vec{e} \right] \quad (51)$$

evaluating Eqn(49) gives

$$\lambda_x = \frac{\partial G}{\partial x} = v_1 (v) + v_2 \left(v^2 - \frac{\mu}{r} + \frac{x^2}{r^3} - \frac{u^2}{\mu} \right) + v_3 \left(\frac{x y}{r^3} - \frac{u v}{\mu} \right) \quad (52a)$$

$$\lambda_y = \frac{\partial G}{\partial y} = v_1 (-u) + v_2 \left(\frac{x y}{r^3} - \frac{u v}{\mu} \right) + v_3 \left(v^2 - \frac{\mu}{r} + \frac{y^2}{r^3} - \frac{v^2}{\mu} \right) \quad (52b)$$

$$\lambda_u = \frac{\partial G}{\partial u} = v_1(-y) + v_2\left(\frac{-y v}{\mu}\right) + v_3\frac{1}{\mu}(2 y u - x v) \quad (52c)$$

$$\lambda_v = \frac{\partial G}{\partial v} = v_1(x) + v_2\frac{1}{\mu}(2 x v - u y) + v_3\left(\frac{-x u}{\mu}\right) \quad (52d)$$

$$\lambda_m = \frac{\partial G}{\partial m} = 1 \quad (52e)$$

note that the constant Lagrange multipliers v_i are additional unknown's.

The last condition deals with the final time. If the final time were free we would use the transversality condition

$$H(\vec{x}(1), \vec{u}(1), \vec{\lambda}(1)) = -\frac{\partial G}{\partial t_f} \quad (52f)$$

or, for this problem

$$H(\vec{x}(1), \vec{u}(1), \vec{\lambda}(1)) = 0 \quad (52g)$$

However, all the solutions presented in this report are fixed-final time. Note, however, that the same algorithm can be used for both types of problems, all that is required is that equation (53g) be replaced by the specification of t_f .

IV.3. Non-Dimensionalization

To improve accuracy, we have non-dimensionalized the problem. This aids in a few ways. First, the integration of the state is more accurate because all variations are on the same order. Second, convergence is improved because all the boundary conditions are immediately placed at or near the same order. Our non-dimensionalized parameters are as follows:

$$\vec{r} \equiv \frac{\vec{r}}{r^*} \quad (53a)$$

$$\vec{V} \equiv \frac{\vec{V}}{\sqrt{\frac{\mu}{r^*}}} \quad (53b)$$

$$\mathbf{m} \equiv \frac{\mathbf{m}}{m^*} \quad (53c)$$

$$t_f \equiv \frac{t_f}{\sqrt{\frac{r^{*3}}{\mu}}} \quad (53d)$$

and they require the following

$$\mathbf{T} \equiv \frac{\mathbf{T}/m^*}{\mu/r^{*2}} \quad (53e)$$

$$(\mathbf{g}_o \mathbf{I}_{sp}) \equiv (\mathbf{g}_o \mathbf{I}_{sp}) \sqrt{\frac{r^*}{\mu}} \quad (53f)$$

$$\mathbf{r}_o \equiv \frac{\mathbf{r}_o}{r^*} \quad (53g)$$

$$\beta \equiv \beta r^* \quad (53h)$$

$$(\rho_o C_{DS}) \equiv (\rho_o C_{DS}) \frac{r^*}{m^*} \quad (53i)$$

$$\mathbf{R} \equiv \frac{\mathbf{R}}{r^*} \quad (53j)$$

The choices of r^* and m^* are completely arbitrary. However, it needs to be said that after a problem is solved by these nondimensionalizations, rescaling must be excersized with caution. This is a direct result of the atmosphere model; if the rescaling is not consistent with the atmosphere model, the results are invalid, e.g. rescaling also rescales the atmosphere model (note Eqn (8)).

If we solve Eqs (53a-j) such that the dimensional parameter is on the left-hand side and then substitute into the original dynamics we find equations that are *exactly* equal to the original equations with $\mu=1$ (The value of J_2 , however, has no dimensions and is not changed). This can be extended to the boundary equations and the costate differential equations. A special note is required for the costates: the costates resulting from the solution to the problem with this transformation will be some scalar multiplied by the 'dimensional' costates, e.g.

$$\vec{\lambda} \equiv \frac{\vec{\lambda}}{\lambda^*} \quad (53k)$$

which requires

$$\vec{v} \equiv \frac{\vec{v}}{\lambda^*} \quad (53l)$$

where λ^* is completely arbitrary. This is easily verified by substitution into the differential equations and boundary conditions.

IV.4. Atmosphere Model

Any atmosphere is usable by simple substitution early in the derivation of the differential constraint. For the purposes of this report we have chosen a very simple atmosphere model. The model is not intended to accurately represent the Earth's atmosphere, or any other planet for that

matter. It is implemented only for the purpose of demonstrating the methods for solving the optimization problem.

Our model is defined at 450km altitude above the planet's equator. The entire atmosphere is assumed isothermal. The temperature is 1000K. The density at the definition altitude is 1.184×10^{-12} kg/m³. This definition point for this model is taken from the 1976 U.S. Standard Atmosphere⁶. The atmosphere is assumed spherical above the oblate planet. For real-world solutions, we strongly recommend the use of the latest standard atmosphere or some appropriate approximation thereof. The contemporary standard atmosphere can be found in ref (7).

IV.5. *The Multiple Point Shooting Method of BOUNDSCO*

One method we are currently using to attempt to solve the TPBVP is the multiple point shooting method. The specific algorithms we are currently using are those given by H. J. Oberle in his subroutine BOUNDSCO⁷, written in FORTRAN. His method, a complete description of which can be found in ref(8), is a modification of the traditional well-known multiple point shooting method.

The use of this method requires the writing of a few routines that define the problem. These routines include, of course, the calling program itself, a subroutine defining the differential constraint (or system dynamics), and a subroutine that defines the constraints on the problem.

The state used in BOUNDSCO differ slightly from the state defined in this report. We have simply adjoined the \vec{v} vector to the state. This requires also that the system dynamics includes a corresponding number of zero derivatives. We justify for this by noting that it allows the statement of the absolute and natural boundary conditions exactly as they are in this report. If we did not implement this, we would have to solve the system of three of the natural boundary conditions for the \vec{v} and substitute the result into the fourth equation, using it in place of the four. This may seem desirable, one equation in the place of four, however, the simple structure of the four

equations is much more desirable than the complex structure of the one equation.

There is one particular feature that makes BOUNDSCO attractive: the explicit inclusion of switching points in the problem formulation. Oberle allows the user to specify the switching function outside of the system dynamics. This simplifies integration and improves convergence. There is a tradeoff; the user must assume a switching structure and verify it outside of BOUNDSCO.

IV.6. The Minimizing-Boundary-Condition Method

The second method we are using is called the Minimizing-Boundary-Condition Method (MBCM)⁸. It is described in ref(9). This method is a modification to the shooting method. It expands the set of available solutions by removing one boundary-condition. The choice of this boundary-condition is arbitrary. Since there is a much larger set of solutions, it is much easier to solve the resulting boundary-value problem. Once this is accomplished, the search for the solution that incorporates the final boundary conditions is treated as a minimization problem. The gradient is numerically calculated and used to update the initial state until the last boundary condition is satisfied. This method is at least as effective as BOUNDSCO in solving the two-point boundary-value problems for the current solved optimal orbit transfers.

The switching structure of optimal control is included in MBCM. The program checks the switching function at each integration step. If the switching function alters sign at one integration step, the program stops the integration and restores all the states to the beginning of the step. A secant method then calculates a smaller step size for integrating the switching function to an exact zero point. From our experience with MBCM some sensitive problems need fourteen digits of accuracy in their switching function. Once the integration passes the switching points the program switches the control and uses a normal step size for integration.

IV.7. Sample Problems and Solutions

Several solutions are presented in this section, all of which both methods were able to converge. As a matter of fact, in most cases, the solution to one problem can be used as the guess to a different problem and the program(s) will converge. All problems have been nondimensionalized and use the atmosphere model presented above.

The first problem presented is a fixed-final-time circle-to-circle orbit transfer:

Find an extremal for the maximum final-mass problem which travels from a circular orbit of $a=3.847$ at $y=3.72$ to another circular orbit of $a=1.5$. The available thrust is (a) 0.9, (b) 0.2 and $g_0 I_{sp}=51.254$. The initial mass is 1.527. The allowed time for transfer is 12.5. $\rho_0 S C_D=3.894 \times 10^{-17}$.

The optimal trajectories are shown in Fig. 1 for $T=0.9$ and in Fig. 3 for $T=0.2$. Their switching functions are shown in Fig. 2 for $T=0.9$ and in Fig. 4 for $T=0.2$.

The second problem presented is a fixed-final-time apse-aligned ellipse-to-ellipse orbit transfer:

Find an extremal for the maximum final-mass problem which travels from an orbit of $a=3.847$ and $r_p=3.756$ at $y=3.76$ to another orbit of $a=1.5$ and $r_p=1$. The apses of the orbits are aligned with the x -axis. The available thrust is (a) 0.9, (b) 0.2 and $g_0 I_{sp}=51.254$. The initial mass is 1.527. The allowed time for transfer is 12. $\rho_0 S C_D=3.894 \times 10^{-17}$.

The optimal trajectories are shown in Fig. 5 for $T=0.9$ and in Fig. 7 for $T=0.2$. Their switching functions are shown in Fig. 6 for $T=0.9$ and in Fig. 8 for $T=0.2$.

The third problem presented is a fixed-final-time non-apse-aligned ellipse-to-ellipse orbit transfer:

Find an extremal for the maximum final-mass problem which travels from an orbit of $a=3.847$ and $r_p=3.756$ at $y=3.76$ to another orbit of $a=1.5$ and $r_p=1$. The apses of the initial orbit is at an angle of 153° with the x -axis, clockwise. The apse of the final orbit is at an angle of 109° with the x -axis, counter-clockwise. The available thrust is (a) 0.9, (b) 0.2 and $g_0 I_{sp}=51.254$. The initial mass is 1.527. The allowed time for transfer is 10. $\rho_0 S C_D=3.894 \times 10^{-17}$.

The optimal trajectories are shown in Fig. 9 for $T=0.9$ and in Fig. 11 for $T=0.2$. Their switching functions are shown in Fig. 10 for $T=0.9$ and in Fig. 12 for $T=0.2$.

V. CONCLUSIONS

The performance of BOUNDSCO was mixed. The ability of the routine to converge solutions is quite strong, however, there is a flaw. BOUNDSCO does not supply information to the user's routine concerning the polarity of the switching function. The user must assume in all his/her code that the desired switching structure is correct. The result of this is that BOUNDSCO often allows itself to converge solutions with inconsistent switching functions. This would not be so bad, except for one other difficulty with BOUNDSCO: the routine does not attempt to aid the user in any way with the initial guess. For example, one finds it nearly impossible to converge a two-burn solution without the insight to guess an initial state that, when integrated, produces two crossings of the switching function (this is actually, not too difficult, if one pays attention to the sign of the switching function and its derivative when making guesses). However, when BOUNDSCO does produce correct solutions, they are as accurate as the user can specify. The solutions presented above satisfy their boundary conditions within 10^{-14} absolute error.

The performance of the minimizing-boundary condition method was also quite promising. This method has one distinct advantage over BOUNDSCO, it explicitly disallows inconsistent switching functions. The method checks the switching function during, but separately from, integration to determine where the switching points are and, most

importantly, what the switching function polarity is. This method is, however, currently a simple shooting method and it exhibits the difficulty of the same. It is expected that if the method is extended to a multiple-point shooting method, it's performance will rival, if not exceed that of BOUNDSCO.

And thereby we come to the recommendation of this study: the development of a method that is a hybrid of multiple-shooting and the minimizing-boundary-condition method.

¹Edelbaum, T.N., "How Many Impulses?" *Aeronautics and Astronautics*, Nov. 1967.

²Anderson, J.D., *Introduction to Flight*, McGraw-Hill Book Co., New York, 1989.

³Anderson, J.D., *Fundamentals of Aerodynamics*, McGraw-Hill Book Co., New York, 1984.

⁴Space Technology Laboratories, *Flight Performance Handbook for Orbital Operations*, Wiley, New York, 1963.

⁵Lawden, D.F., *Optimal Trajectories for Space Navigation*, Butterworths, London, 1963.

⁶COESA, *U.S. Standard Atmosphere, 1976*, U.S. Government Printing Office, Washington, D.C. 1976

⁷Oberle, H. J., BOUNDSCO - Hinweise zur Benutzung des Mehrzielverfahrens für die numerische Lösung von Randwertproblemen mit Schaltbedingungen, *Hamburger Beiträge zur Angewandten Mathematik, Berichte 6*, 1987.

⁸Chuang, C.-H., and Speyer, J.L., "Periodic Optimal Hypersonic Scramjet Cruise," *Optimal Control Applications & Methods*, Vol. 8, pp. 231-242 (1987)

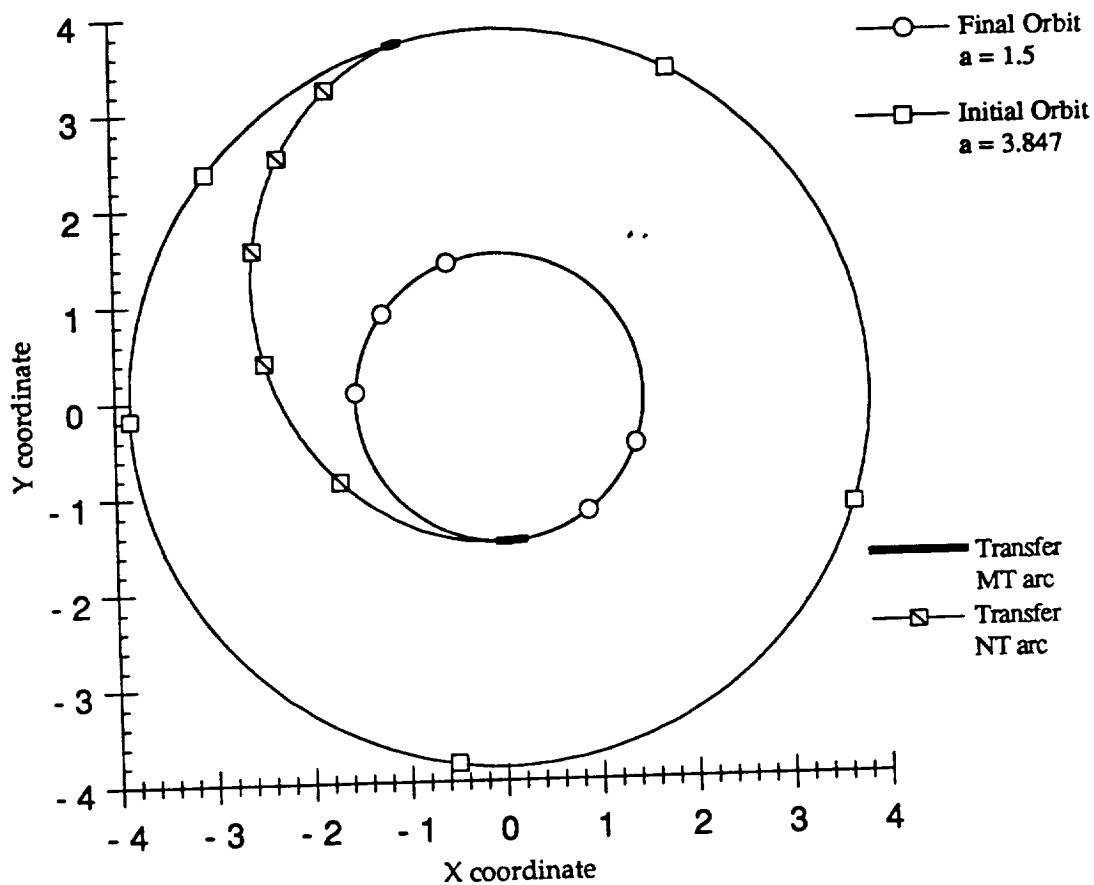


Fig 1 Mass-Optimal Circle-to-Circle Orbit Transfer, $T=0.9$

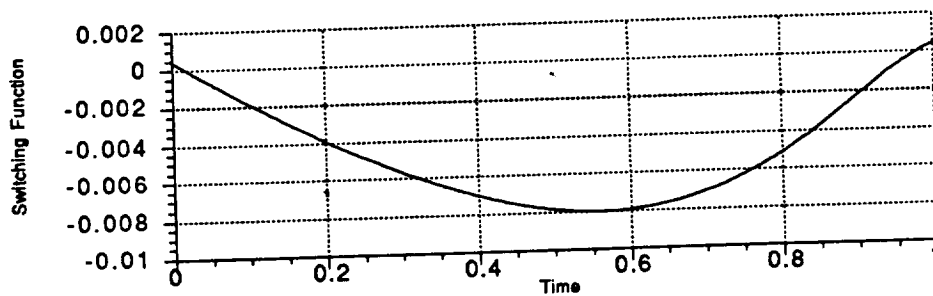


Fig. 2 Graph of Switching Function Corresponding to Figure 1, $T=0.9$

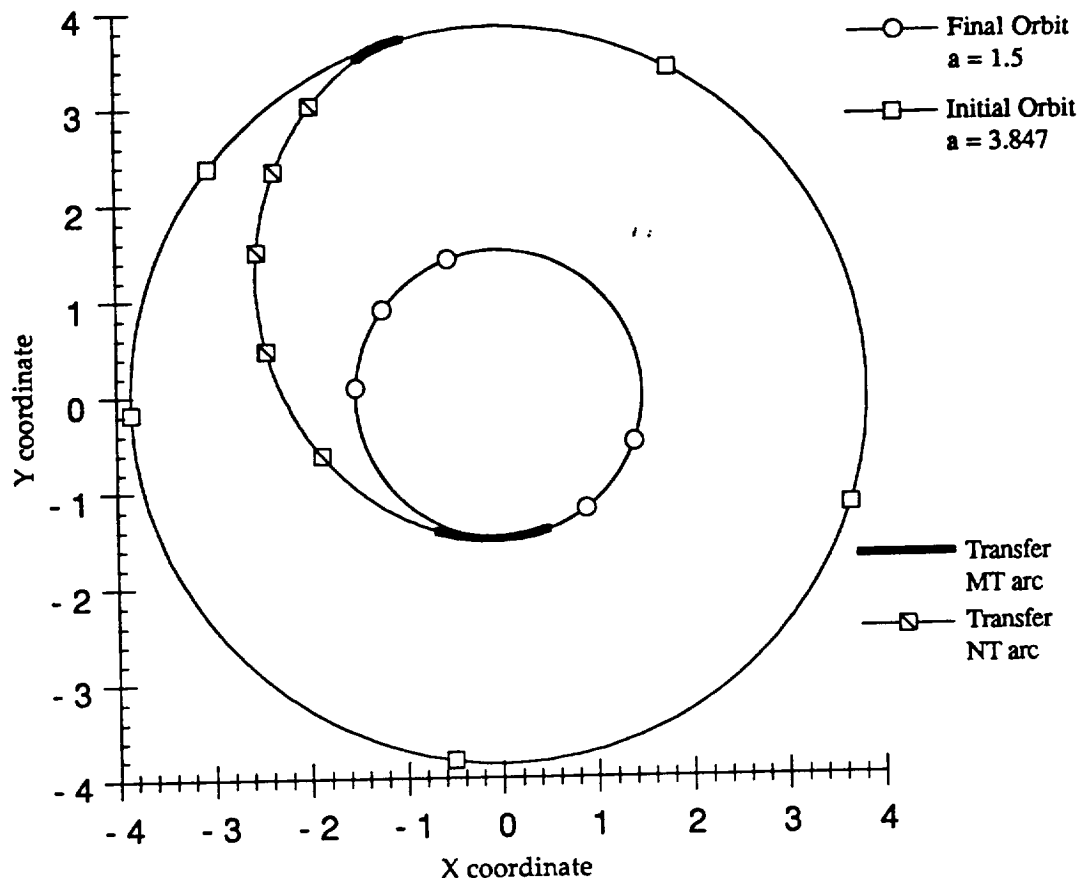


Fig 3 Mass-Optimal Circle-to-Circle Orbit Transfer, $T=0.2$

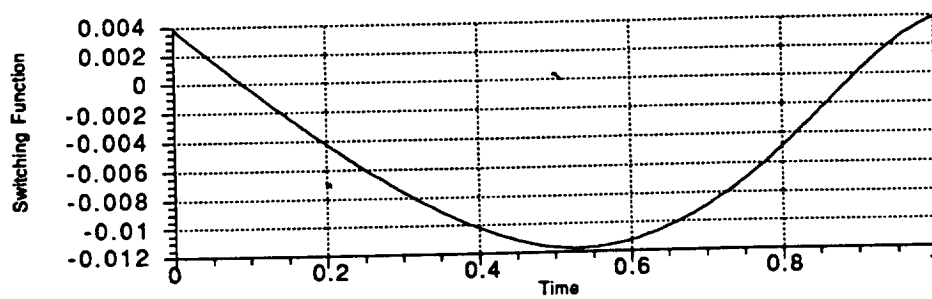


Fig. 4 Graph of Switching Function Corresponding to Figure 3, $T=0.2$

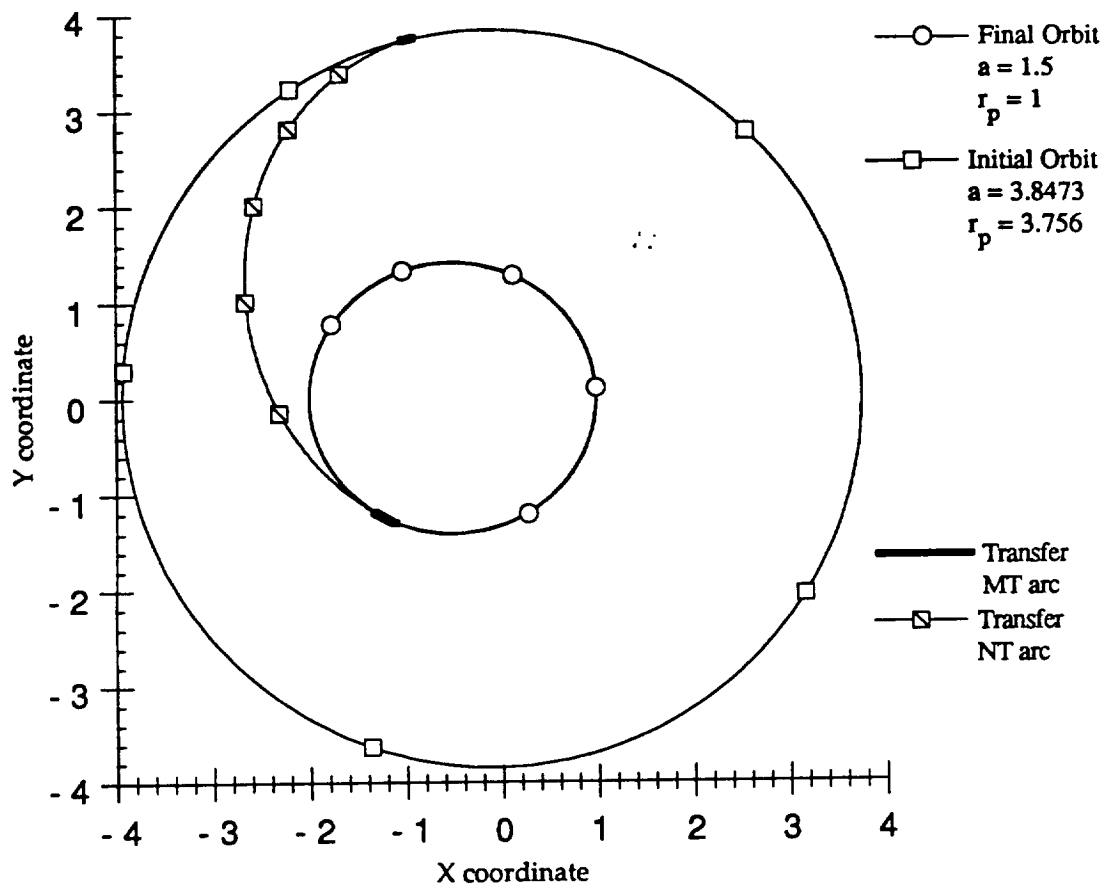


Fig. 5 Mass-Optimal Aligned-Ellipse-to-Ellipse Orbit Transfer, $T=0.9$

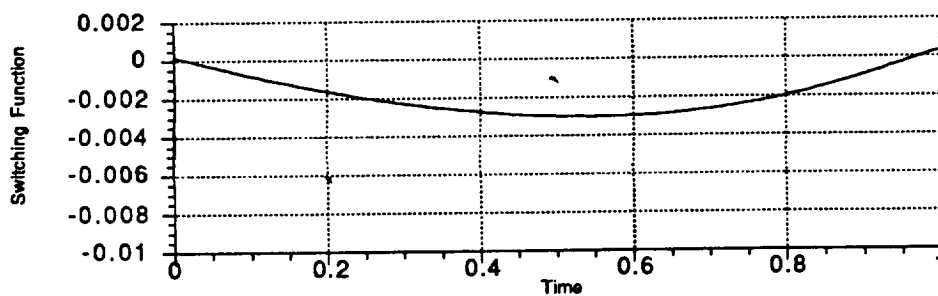


Fig. 6 Graph of Switching Function Corresponding to Figure 5, $T=0.9$

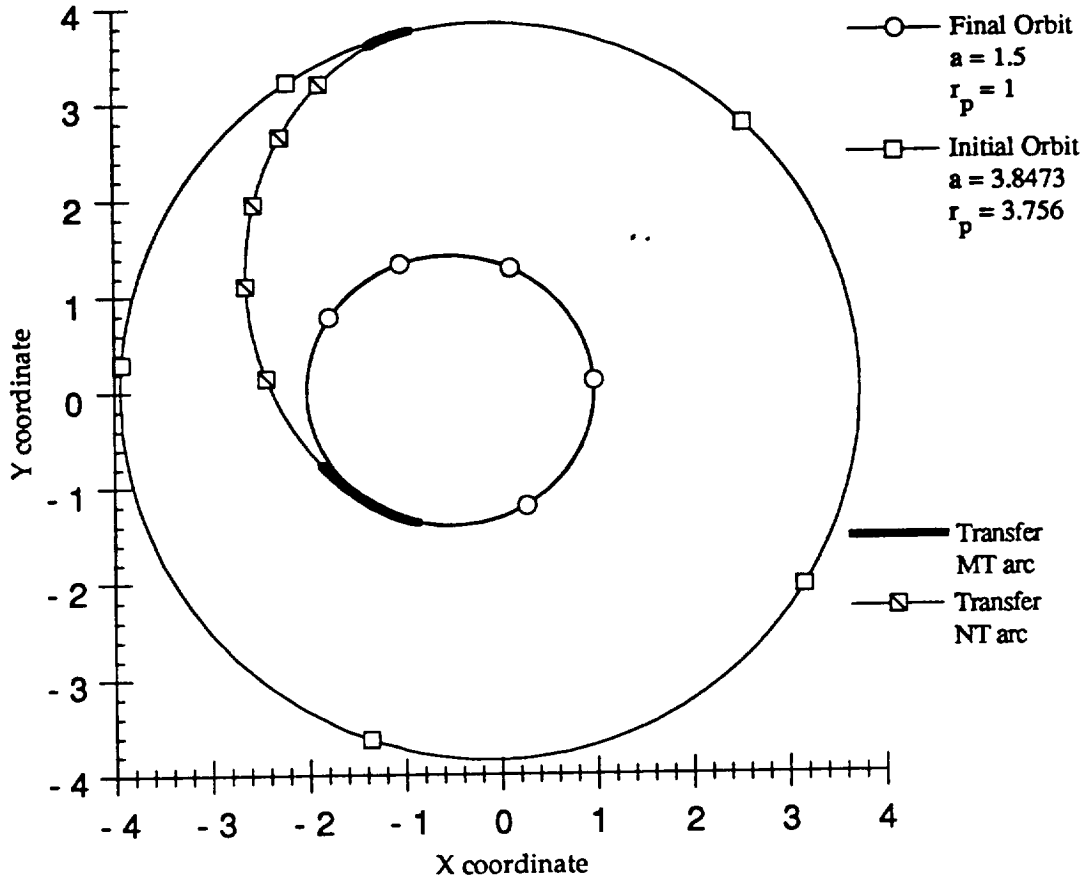


Fig. 7 Mass-Optimal Aligned-Ellipse-to-Ellipse Orbit Transfer, $T=0.2$

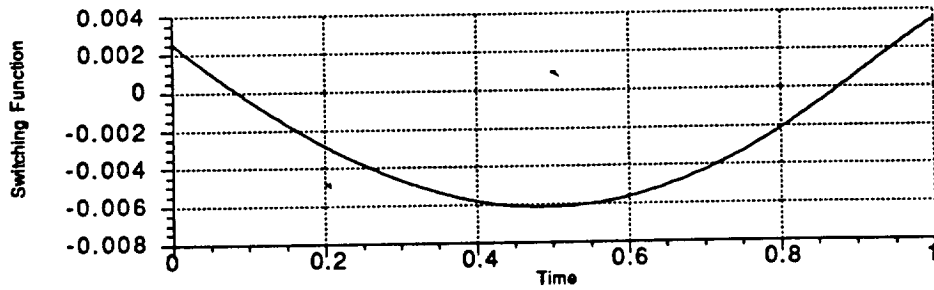


Fig. 3 Graph of Switching Function Corresponding to Figure 7, $T=0.2$

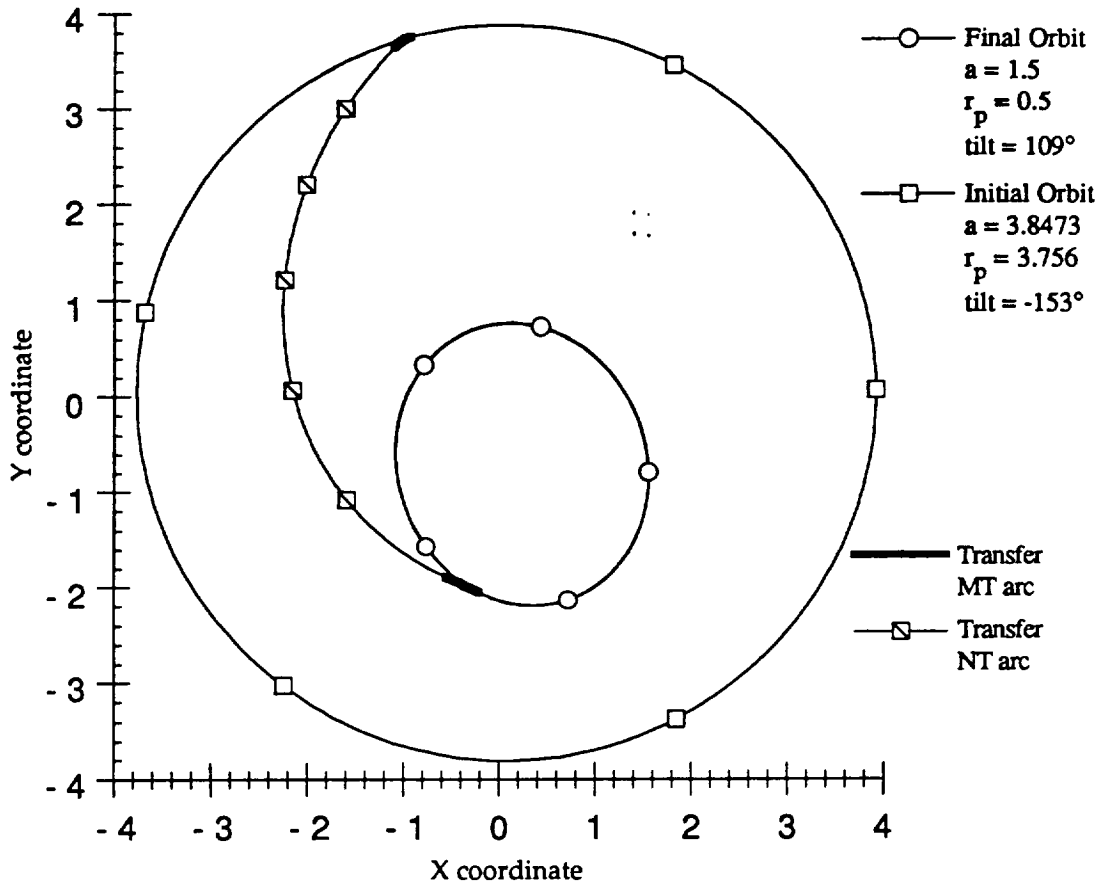


Fig. 9 Mass-Optimal Non-Aligned-Ellipse-to-Ellipse Orbit Transfer, $T=0.9$

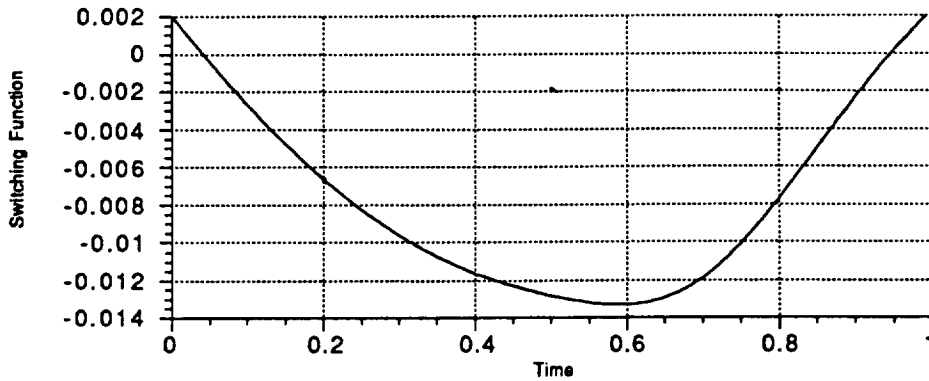


Fig. 10 Graph of Switching Function Corresponding to Figure 9, $T=0.9$

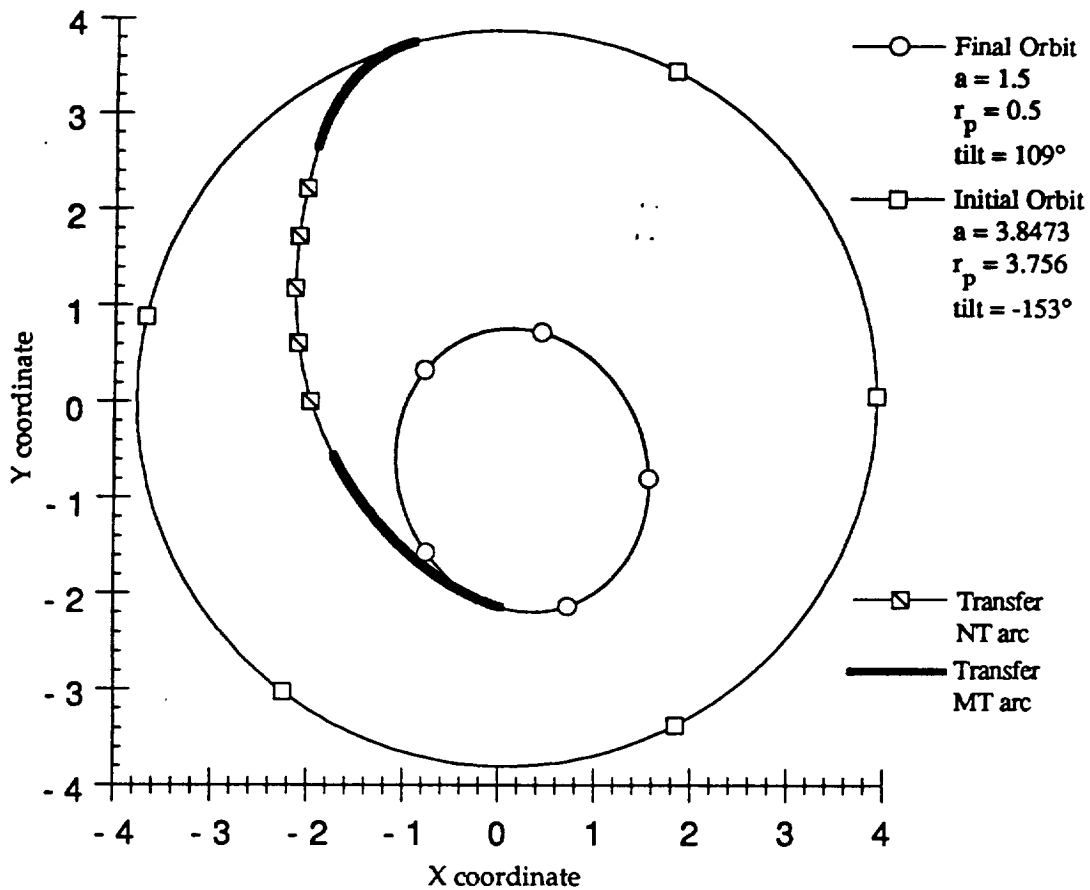


Fig. 11 Mass-Optimal Non-Aligned-Ellipse-to-Ellipse Orbit Transfer, T=0.2

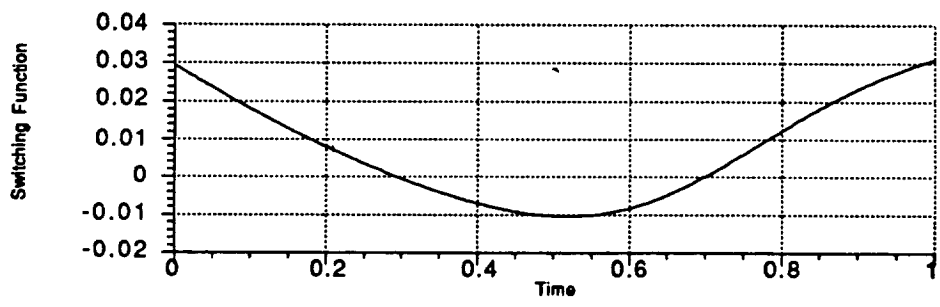


Fig. 12 Graph of Switching Function Corresponding to Figure 11, T=0.2